Asian Journal of Research and Reviews in Physics

2(4): 1-18, 2019; Article no.AJR2P.52078

Study of (p,n) Reaction in a Wide Energy Range

N. A. El-Nohy[1], M. N. El-Hammamy[2*], S. Diab[1] and A. M. El-Shinawy[1]

[1]Department of Physics, Faculty of Science, Alexandria University, Alexandria, Egypt.
[2]Department of Physics, Faculty of Science, Damanhur University, Damanhur, Egypt.

Authors' contributions

This work was carried out in collaboration among all authors. Authors NAEN and MNEH designed the study, performed the statistical analysis, wrote the protocol and wrote the first draft of the manuscript. Authors AMES and SD managed the analyses of the study. Author AMES managed the literature searches. All authors read and approved the final manuscript.

Article Information

DOI: 10.9734/AJR2P/2019/v2i430107
Editor(s):
(1) Dr. Vitalii A. Okorokov, Professor, Department of Physics, National Research Nuclear University MEPhI (Moscow Engineering Physics Institute) – NRNU MEPhI, Moscow, Russia.
Reviewers:
(1) Roberto Arceo, Autonomous University of Chiapas, Mexico.
(2) Sugie Shim, Kongju National University, South Korea.
(3) A. Ayeshamariam, Khadir Mohideen College, India.
Complete Peer review History: https://sdiarticle4.com/review-history/52078

Original Research Article

Received 13 August 2019
Accepted 22 October 2019
Published 06 November 2019

ABSTRACT

In this paper, the quasi-elastic scattering (p, n) reactions are studied for a wide range of target nuclei ^{13}C, ^{14}C, ^{48}Ca, ^{90}Zr and ^{208}Pb and different incident energies (35-160 MeV). The phenomenological Optical model potential and density independent approaches are used for these calculations in comparison with density dependent semi-microscopic approach. The density dependent parameters are modified to achieve the best calculations for many targets at different energy levels.

Keywords: Quasi-elastic scattering; single folding; lane potential.

PACS: 24.50.+g, 25.60.Bx, 25.60.Lg

1. INTRODUCTION

Examinations of the elastic and quasi-elastic scattering of neutrons and protons is one simplest way for better understanding the character of the nuclear interaction. The isospin is one important and interesting feature of the nucleon-nucleus interactions. In order to be

**Corresponding author: E-mail: marwa1374@yahoo.com;*

determined, Lane [1] postulated a straightforward reliance of the nucleon-nucleus optical potential upon the isospin operators in terms of the optical model (OM). The matrix elements ensuing from this dependence are expressed in simple forms [2] for both of the (p,p), (n,n), and the (p,n) reactions.

Also, more realistic method is using the folded nucleon-nucleon (NN) interaction potential in the framework of OM. The folded potential represents the real part of the optical potential [3-5]. Within this method, antisymmetrization of the investigated system has been mulled over to incorporate the exchange terms [6].

We represent here a systematic study of the (p,n) reactions in the framework of the OM, in which the interaction potential is engendered by folding the chosen potential with the densities of the nucleus. The NN interactions are taken in the form of sums of direct and zero range exchange terms. Supplementally, phenomenological OM is used to describe the same reactions. It is an extending to our previous work [7].

2. THE LANE MODEL

The nuclear interaction between an incident nucleon and a target with non-zero isospin has an isospin dependent part. The lane isospin dependent part is formulated as

$$\frac{4tT}{A}U_1 \quad , \tag{1}$$

where, U_1 is known as the Lane potential that contributes to both the elastic (p,p) and (n,n) scattering just as to the charge exchange (p,n) reaction. The isospin of the particle and target nucleus, are t, T, respectively and A is the mass number of the target. Thus, in a straightforward method, lane potential (isospin dependent part) is connected to optical potential to form the total nuclear nucleon-nucleus interaction as

$$U = U_o + \frac{4tT}{A}U_1 \quad . \tag{2}$$

Knowledge of U_1 is of key enthusiasm for investigations of nuclear phenomena in which neutrons and protons are different (isovector modes). Numerous past appraisals of U_1 are liable to serious uncertainties as Distorted Wave Born Approximation (DWBA) analysis of (p,n) reactions. For instance, in the comparison of elastic nucleon scattering from different nuclei one must make assumptions [2] about the variation of nuclear geometry with A and ε $\left(\varepsilon = \frac{N-Z}{A}\right)$. It is on a fundamental level conceivable to stay away from these uncertainties by extracting U_1 from a consistent study of the elastic proton and neutron scattering and the charge exchange (p,n) reaction on the same target nucleus, at the same energy. We recall here briefly the consistent isospin coupling scheme [1] for the elastic nucleon-nucleus scattering and charge exchange (p,n) reaction exciting.

The matrix elements resulting from equation (2) give the following relationships [2].

$$U_{pp} = U_o - \frac{N-Z}{A}U_1 \tag{3}$$

$$U_{nn} = U_o + \frac{N-Z}{A}U_1 \tag{4}$$

Similarly, the transition matrix element or (p,n) form factor for the charge exchange reaction is

$$U_{pn} = \frac{2(N-Z)^{1/2}}{A}U_1 \tag{5}$$

Accordingly

$$U_{nn} - U_{pp} = \frac{2(N-Z)}{A}U_1 = (N-Z)^{1/2}U_{pn} \quad . \tag{6}$$

The present calculations of angular distributions of the (p,n) elastic scattering cross sections were made by using the distorted-wave code DWUCK4 [8], and the optical potential is

$$U_{pp(nn)}(R) = N_R\left[V_{F0}(R) \pm \frac{N-Z}{A}V_{F1}(R)\right] + iW(R) \quad , \tag{7}$$

For (n,n) , (p,p), and for (p,n) reaction

$$U_{pn}(R) = \frac{2(N-Z)^{1/2}}{A}\left[N_R V_{F1}(R) + iW(R)\right] \quad , \tag{8}$$

where $V_{F0(1)}$ (R) is the nuclear real potential calculated by the folding procedure, including the zero range exchange part of the potential by using DFPOT code [9]. W(R) is the imaginary part of the potential including both type; volume W_V(R) and surface W_S(R).

The last outcomes for the angular distributions of scattering cross sections were gotten by changing the parameters of the imaginary part of the potential to get the best fit with the experimental values.

3. METHOD OF CALCULATIONS

In this work, we study the quasi-elastic scattering (p,n) reaction. Differential scattering cross sections are determined for a wide range of incident proton energies by different targets. Initially, proton of energies 35, 45 and 135 MeV [10,11,12] incident on target nuclei ^{48}Ca. Pursued by, proton of energies 35, 45, 120 and 160 MeV [10,13,14] incidents on target nuclei ^{90}Zr. Then, proton of energies 35 and 45 MeV [9] incidents on target nucleus ^{208}Pb. At long last, proton of energies 35 and 120 MeV [15,16] incidents on target isotope nuclei ^{13}C and ^{14}C, respectively.

3.1 The Phenomenological Optical Potential

The global WS parameters for different nucleon potentials [17-19] have been carefully determined based on large experimental data bases of the elastic nucleon-nucleus scattering. Then, it has been found to be useful in calculation of the transition optical potential (Upn).

We have been chosen CH89 global optical parameters as initial parameters, and in that case a minor change is needed to reproduce the best fit of the scattering cross sections with the experimental data in the optical model (OM) analysis. The equations and parameters used in potential CH89 are listed in ref. [18].

3.2 Density Independence Folding Potential

The nucleon-nucleus potential can be obtained by single folding (SF) the density distribution of the target nucleus $\rho_T(r)$ with the NN effective interaction V_{NN} (S) [20]

$$V_F(R) = \int \rho_T(r)\, V_{NN}(S)\, dr \quad , \qquad (9)$$

where, $S = |R - r|$ is the distance between the two nucleons. Here, we take the NN interaction to be density independent (DI) M3Y effective NN interaction with a zero–range approximation in the form

$$(V_0)_{NN}(S) = 7999\frac{e^{-4s}}{4s} - 2134\frac{e^{-2.5s}}{2.5s} - 276[1-\alpha\varepsilon]\,\delta(s) \qquad (10)$$

and

$$(V_1)_{NN}(S) = -4886\frac{e^{-4s}}{4s} + 1176\frac{e^{-2.5s}}{2.5s} + 228[1-\alpha\varepsilon]\,\delta(s) \quad . \qquad (11)$$

V_0 and V_1 are the (isoscalar and isovector) M3Y effective NN interaction potential respectively, supplemented by zero range potentials. Where (α) is the energy dependent parameter = 0.005 MeV^{-1}.The zero range potential (third term) in equations (10) and (11) represents the single nucleon exchange term [20].

Consequently, the real folded isoscalar *V_{F0} (R)* and isovector *V_{F1} (R)* components of *V_F (R)* potentials are calculated and further scaled by a factor N_R in addition to W(R) to obtain $U_{0(1)}$. Thus, the best fitted real folded potential in addition to WS imaginary potential parameters is listed in Tables 1-11.

3.3 Density Dependence Folding Potential

The failure of simple M3Y-NN type interactions to give a good description of the data in many cases [21-24], leads to the inclusion of explicit density dependence. In consequence, the other type (DD) of the SF potential is introduced as follow

$$V_F(R) = g(\rho,\varepsilon)\int \rho_T(r)\, V_{NN}(S)\, dr \quad . \qquad (12)$$

The density dependence [25] adopted is

$$g(\rho,\varepsilon) = C(1-\beta(\varepsilon)\,\rho^n)\ . \qquad (13)$$

The density dependent parameters C and β, can be given by the subsequent

$$\beta = \left[(1-P)\rho_\circ^{-n}\right]\left[(3n+1)-(n+1)P\right]^{-1} \quad , (14)$$

$$P = (10m\varepsilon_\circ)\left(\hbar^2 k_\circ^2\right)^{-1} \quad , \qquad (15)$$

$$k_\circ = \left[1.5\pi^2 \rho_\circ\right]^{1/3}, \quad (16)$$

$$C = -\left(2\hbar^2 k_\circ^2\right)\left[5mJ_\circ \rho_\circ \left(1-(n+1)\rho_\circ^n \beta\right)\right]^{-1}, \quad (17)$$

Where m is a nucleonic mass equal to 931.5 MeV/c^2, k_o is Fermi momentum at saturation condition. It is quite obvious that density dependence parameter (β) obtained by this method depends only on the saturation energy per nucleon ($\varepsilon_\circ$), the saturation density (ρ_0) and the index (n) but not on the parameters of the M3Y interaction while the parameter (C) depends on and also through the volume integral ($J_\circ$) of the isosaclar part of the M3Y interaction supplemented by the zero range exchange potential having the form

$$J_\circ = \int (V_\circ)_{NN}(S)\, d^3S \quad . \quad (18)$$

As a result, the two parameters β and C are chosen to have different values with different investigated energies. Thus, the density dependent factor g(ρ,ε) is turned out to be function of energy. The value of parameter n= 2/3 was firstly taken by Myers in the SF calculation [25]. Three forms are applied in our analysis which is summarized according to energy range used as:

$$g(\rho,\varepsilon) = 2.07(1- 1.667\ \rho^{2/3}) \quad (19)$$

this is denoted as DD1 within energy range 120-160 MeV, where $\rho_0 = 0.15$ [26,27],

$$g(\rho,\varepsilon) = 2.85(1- 1.614\ \rho^{2/3}) \quad (20)$$

this is indicated as DD2 at energy 45 MeV, where $\rho_0 = 0.16$ [28,29], and

$$g(\rho,\varepsilon) = 1.55(1- 1.054\ \rho^{2/3}), \quad (21)$$

this is referred to as DD3 at energy 35 MeV, where $\rho_0 = 0.28$ [30,31].

Notice that, g(ρ,ε) in equation (13) is a function of energy at only one value at saturation. Then, it was our trial to be obtained as a variable function with changing energy. According to the investigated results, it is appropriate to improve the value of ρ_0 to be as a function in energy to generalize and achieve the three ranges. This is represented by:

$$\rho_\circ = 10^{-8}E^4 - 5\times10^{-6}E^3 + 8\times10^{-4}E^2 - 0.058E + 1.47 \quad . \quad (22)$$

Consistent with the above formula, it is proper to draw the relation that shows the variation of ρ_0 with E in the Fig. 1 as following:

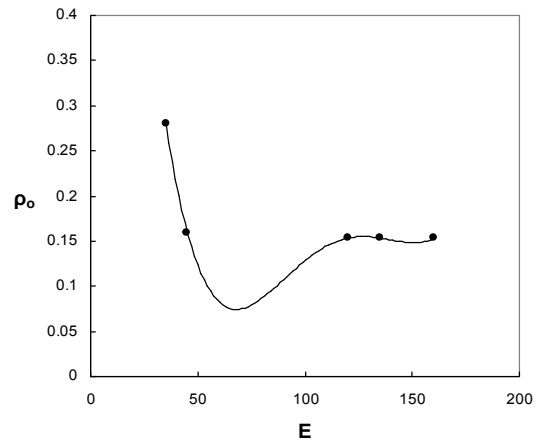

Fig. 1. The variation of different values of saturation density (ρ_0) with different energies (E)

Summarizing that, we are used the SF program to calculate the real parts of the nucleon-nucleus scattering of several systems. The interactions are divided into density independence M3Y-DI and density dependence DD1, DD2 and DD3 interaction. From the above description, the basic inputs to a folding calculation are nuclear densities of the target nuclei and the effective NN interaction. The densities of ^{13}C and ^{14}C are taken as Gaussian [32], ^{48}Ca [33], ^{90}Zr [34] and ^{208}Pb [35] are taken as Fermi. In the present work, we examine a few representative cases about the real part of nuclear potential. These data are very helpful to test the modified density dependent Folding potential.

4. RESULTS AND DISCUSSION

In this work, the phenomenological OM and semi-microscopic (SF) model are used. The DI and DD1, DD2 and DD3 effective NN interaction is employed to drive the real folding optical model potentials of the investigated systems, assuming the density distribution for different targets nuclei. The imaginary potentials are supplemented to the derived potentials in phenomenological Woods-Saxon (WS) form. The quasi-elastic angular distributions for the different systems are calculated and the results are compared to the experimental data.

Table 1. The best-fit parameters of the folded real potential in addition to Woods-Saxon imaginary potentials to (p,n) data of ^{90}Zr at 35 MeV within different models

Model	Channel	N_R	V MeV	r fm	a fm	W_v MeV	R_v fm	a_v fm	W_s MeV	R_s Fm	a_s fm
OM	(p,p)	-	70.97	1.062	0.8563	0.966	1.47	0.69	6.785	1.27	0.69
	(n ,n)	-	14.21	1.052	0.8454	0.696	1.27	0.69	5.878	1.27	0.69
	(p,n)	-	1.73	1.045	0.8795	1.326	1.16	0.69	0.00	0.00	0.00
DI	(p,p)	2.64	66.97	1.0427	0.8263	0.166	1.37	0.69	6.785	1.27	0.69
	(n ,n)	0.53	12.21	1.0427	0.8254	0.096	1.27	0.69	5.878	1.27	0.69
	(p,n)	2.30	1.830	1.0356	0.8595	1.366	1.17	0.69	0.00	0.00	0.00
DD1	(p,p)	1.86	71.97	1.0429	0.8263	0.866	1.47	0.69	6.785	1.27	0.69
	(n ,n)	0.41	14.21	1.0427	0.8254	0.596	1.27	0.69	5.878	1.27	0.69
	(p,n)	1.59	1.930	1.0360	0.8622	1.356	1.17	0.99	0.00	0.00	0.00
DD3	(p,p)	2.10	75.00	1.0427	0.8294	0.966	1.37	0.69	6.785	1.27	0.69
	(n ,n)	0.53	15.81	1.0431	0.8256	0.956	1.37	0.69	5.878	1.27	0.69
	(p,n)	1.89	1.930	1.0358	0.8611	1.206	1.17	0.69	0.00	0.00	0.00

Table 2. The best-fit parameters of the folded real potential in addition to Woods-Saxon imaginary potentials to (p,n) data of ^{90}Zr at 45 MeV within different models

Model	Channel	N_R	V MeV	r fm	a fm	W_v MeV	R_v fm	a_v fm	W_s MeV	R_s Fm	a_s fm
OM	(p,p)	-	68.72	1.049	0.8431	3.052	1.27	0.69	5.974	1.27	0.69
	(n ,n)	-	23.62	1.050	0.8380	3.080	1.27	0.69	5.098	1.27	0.69
	(p,n)	-	1.277	1.038	0.8875	1.152	1.29	0.69	0.00	0.00	0.00
DI	(p,p)	0.83	69.72	1.0391	0.8431	3.052	1.27	0.69	5.974	1.27	0.69
	(n ,n)	0.29	22.62	1.0402	0.8380	3.080	1.27	0.69	5.098	1.27	0.69
	(p,n)	0.46	1.177	1.0289	0.8875	1.152	1.29	0.69	0.00	0.00	0.00
DD1	(p,p)	1.11	75.72	1.0425	0.8467	6.052	1.27	0.69	5.974	1.27	0.69
	(n ,n)	0.42	25.62	1.0431	0.8421	4.080	1.27	0.69	5.098	1.27	0.69
	(p,n)	0.75	1.557	1.0324	0.8932	1.552	1.27	0.69	0.00	0.00	0.00
DD2	(p,p)	0.75	73.72	1.042	0.8466	6.052	1.27	0.99	5.97	1.27	0.69
	(n ,n)	0.28	24.62	1.0431	0.8412	4.080	1.27	0.99	5.09	1.27	0.69
	(p,n)	0.56	1.677	1.0322	0.8928	1.502	1.28	0.69	0.00	0.00	0.00

Table 3. The best-fit parameters of the folded real potential in addition to Woods-Saxon imaginary potentials to (p,n) data of ^{90}Zr at 120 MeV within different models

Model	Channel	N_R	V MeV	r fm	a fm	W_v MeV	R_v fm	a_v fm	W_s MeV	R_s Fm	a_s fm
OM	(p,p)	-	52.56	0.9663	1.057	7.73	1.27	0.69	1.338	1.27	0.69
	(n ,n)	-	31.84	1.203	0.9018	7.76	1.27	0.69	1.123	1.27	0.69
	(p,n)	-	1.905	0.885	1.277	0.38	1.27	0.69	0.00	0.00	0.00
DI	(p,p)	0.83	50.16	0.9963	1.007	7.730	1.27	0.69	1.388	1.27	0.69
	(n ,n)	0.55	30.59	1.0039	0.9818	7.760	1.27	0.69	1.123	1.27	0.69
	(p,n)	1.38	1.885	0.8557	1.377	0.430	1.27	0.69	0.00	0.00	0.00
DD1	(p,p)	1.25	50.16	0.9514	1.166	7.730	1.27	0.69	1.388	1.27	0.69
	(n ,n)	0.84	30.59	0.9584	1.146	7.760	1.57	0.69	1.123	1.27	0.69
	(p,n)	1.79	1.985	0.8588	1.394	0.350	1.27	0.69	0.00	0.00	0.00

Table 4. The best-fit parameters of the folded real potential in addition to Woods-Saxon imaginary potentials to (p,n) data of ^{90}Zr at 160 MeV within different models

Model	Channel	N_R	V MeV	r fm	a fm	W_v MeV	R_v fm	a_v fm	W_s MeV	R_s Fm	a_s fm
OM	(p,p)	-	60.50	0.951	1.273	5.794	1.27	0.99	0.509	1.27	0.69
	(n ,n)	-	38.81	0.951	1.158	8.196	2.27	0.59	0.406	1.27	0.69
	(p,n)	-	0.456	0.965	2.646	1.124	1.17	0.99	0.00	0.00	0.00
DI	(p,p)	0.96	61.90	0.9414	1.173	5.794	1.27	0.99	0.509	1.27	0.69
	(n ,n)	0.58	35.41	0.961	1.118	8.196	2.27	0.59	0.406	1.27	0.69
	(p,n)	0.06	0.356	0.955	2.546	1.124	1.17	0.89	0.00	0.00	0.00
DD1	(p,p)	1.59	55.90	0.9476	1.198	8.794	0.17	0.99	0.509	1.27	0.69
	(n ,n)	1.06	35.41	0.9673	1.140	8.196	0.37	0.69	0.406	1.27	0.69
	(p,n)	0.008	0.146	2.249	2.805	0.694	1.10	0.99	0.00	0.00	0.00

Table 5. The best-fit parameters of the folded real potential in addition to Woods-Saxon imaginary potentials to (p,n) data of ^{13}C at 35 MeV within different models

Model	Channel	N_R	V MeV	r fm	a fm	W_v MeV	R_v fm	a_v fm	W_s MeV	R_s Fm	a_s fm
OM	(p,p)	-	65.58	0.694	0.631	1.238	1.25	0.49	4.490	1.15	0.69
	(n ,n)	-	55.82	0.692	0.630	1.600	1.25	0.69	5.769	1.65	0.69
	(p,n)	-	0.784	0.635	0.658	2.700	1.43	1.10	0.00	0.00	0.00
DI	(p,p)	0.64	50.58	0.7944	0.7314	1.238	1.25	0.49	4.490	1.15	0.69
	(n ,n)	0.62	45.82	0.7927	0.7300	1.600	1.25	0.69	5.769	1.65	0.69
	(p,n)	0.12	0.584	0.8254	0.7389	2.700	1.44	0.95	0.00	0.00	0.00
DD1	(p,p)	0.66	48.98	0.8084	0.7315	1.638	0.55	0.69	4.49	1.15	0.69
	(n ,n)	0.65	45.02	0.8059	0.7309	1.600	2.55	0.69	5.76	1.15	0.69
	(p,n)	0.17	0.784	0.8505	0.7359	5.638	1.05	0.89	0.00	0.00	0.00
DD3	(p,p)	0.83	42.98	0.9530	0.7434	1.638	1.55	0.69	4.49	1.15	0.69
	(n ,n)	0.82	40.02	0.9488	0.7439	1.600	1.55	0.69	5.76	1.15	0.69
	(p,n)	0.09	0.284	1.0058	0.7393	6.638	0.98	0.89	0.00	0.00	0.00

Table 6. The best-fit parameters of the folded real potential in addition to Woods-Saxon imaginary potentials to (p,n) data of ^{14}C at 120 MeV within different models

Model	Channel	N_R	V MeV	r fm	a fm	W_v MeV	R_v fm	a_v fm	W_s MeV	R_s Fm	a_s fm
OM	(p,p)	-	39.50	1.255	0.650	8.756	1.25	0.69	1.239	1.15	0.69
	(n ,n)	-	22.50	1.177	0.669	5.761	1.25	0.69	0.936	1.15	0.69
	(p,n)	-	0.097	1.840	0.256	3.856	0.87	0.79	0.00	0.00	0.00
DI	(p,p)	1.22	35.50	1.1559	0.6001	8.756	1.25	0.69	1.239	1.15	0.69
	(n ,n)	0.67	20.50	1.0776	0.6494	5.761	1.25	0.69	0.936	1.15	0.69
	(p,n)	0.17	0.067	1.8409	0.2167	3.856	0.87	0.79	0.00	0.00	0.00
DD1	(p,p)	1.01	29.50	1.1551	0.6013	8.756	1.25	0.69	1.239	1.15	0.69
	(n ,n)	1.00	30.50	1.0775	0.6481	5.761	1.25	0.69	0.936	1.55	0.69
	(p,n)	0.25	0.097	1.8413	0.2216	3.856	0.87	0.79	0.00	0.00	0.00

Table 7. The best-fit parameters of the folded real potential in addition to Woods-Saxon imaginary potentials to (p,n) data of ^{48}Ca at 35 MeV within different models

Model	Channel	N_R	V MeV	r fm	a fm	W_v MeV	R_v fm	a_v fm	W_s MeV	R_s Fm	a_s fm
OM	(p,p)	-	36.16	1.158	0.69	3.27	1.11	0.69	7.073	1.11	0.69
	(n ,n)	-	32.79	1.158	0.69	3.90	1.11	0.69	3.420	1.11	0.69
	(p,n)	-	1.100	1.158	0.69	3.42	1.21	0.69	0.00	0.00	0.00
DI	(p,p)	1.08	70.27	0.9870	0.8826	2.270	1.21	0.69	7.073	1.11	0.69
	(n ,n)	0.64	35.85	0.9881	0.8782	2.900	1.21	0.69	3.420	1.11	0.69
	(p,n)	0.67	2.230	0.9779	0.9128	2.270	1.21	0.60	0.00	0.00	0.00
DD1	(p,p)	0.88	60.12	0.9966	0.8986	6.110	1.11	0.69	8.073	1.11	0.69
	(n ,n)	0.88	51.29	0.9977	0.8934	8.900	1.11	0.69	7.420	1.11	0.69
	(p,n)	0.25	0.882	0.9875	0.9304	4.100	1.21	0.55	0.00	0.00	0.00
DD3	(p,p)	0.89	62.12	0.9911	0.8905	4.510	1.11	0.69	0.173	1.11	0.69
	(n ,n)	0.76	45.29	0.9927	0.8849	8.110	1.11	0.69	5.42	1.11	0.69
	(p,n)	0.28	0.982	0.9820	0.9215	2.900	1.25	0.59	0.00	0.00	0.00

Table 8. The best-fit parameters of the folded real potential in addition to Woods-Saxon imaginary potentials to (p,n) data of ^{48}Ca at 45 MeV within different models

Model	Channel	N_R	V MeV	r fm	a fm	W_v MeV	R_v fm	a_v fm	W_s MeV	R_s Fm	a_s fm
OM	(p,p)	-	56.46	0.964	0.7512	1.184	1.21	0.69	6.163	1.11	0.69
	(n ,n)	-	41.81	0.924	0.9207	1.18	1.21	0.69	5.383	1.11	0.69
	(p,n)	-	0.145	1.054	0.1445	2.88	1.25	0.69	0.00	0.00	0.00
DI	(p,p)	0.89	60.46	0.9647	0.7812	1.184	1.21	0.69	6.163	1.11	0.69
	(n ,n)	0.62	40.81	0.9248	0.9107	1.180	1.21	0.69	5.383	1.11	0.69
	(p,n)	0.16	0.245	1.0549	0.1345	2.880	1.10	0.69	0.00	0.00	0.00
DD1	(p,p)	0.97	62.16	0.9724	0.7934	1.770	1.21	0.69	6.163	1.11	0.69
	(n ,n)	0.64	39.79	0.9319	0.9309	1.280	1.21	0.69	5.420	1.11	0.69
	(p,n)	0.14	0.200	1.0566	0.1329	2.520	1.21	0.69	0.00	0.00	0.00
DD2	(p,p)	0.57	48.16	1.040	06966	0.770	0.85	0.39	6.163	1.11	0.69
	(n ,n)	0.52	42.09	1.026	0.8091	2.780	1.21	0.69	5.42	1.11	0.69
	(p,n)	0.09	0.20	1.0563	0.1331	4.520	1.00	0.89	0.00	0.00	0.00

Table 9. The best-fit parameters of the folded real potential in addition to Woods-Saxon imaginary potentials to (p,n) data of ^{48}Ca at 135 MeV within different models

Model	Channel	N_R	V MeV	r fm	a fm	W_v MeV	R_v fm	a_v fm	W_s MeV	R_s Fm	a_s fm
OM	(p,p)	-	40.16	1.158	0.69	2.27	1.11	0.69	7.073	1.11	0.69
	(n ,n)	-	20.79	1.158	0.69	2.90	1.11	0.69	3.420	1.11	0.69
	(p,n)	-	0.100	1.158	0.69	1.22	1.11	0.79	0.00	0.00	0.00
DI	(p,p)	1.27	60.80	0.8755	1.041	2.77	1.11	1.19	0.950	1.11	0.69
	(n ,n)	0.68	30.10	0.8917	0.997	7.780	1.21	0.89	0.449	1.11	0.69
	(p,n)	0.06	0.10	0.4344	1.785	1.670	1.01	0.79	0.00	0.00	0.00
DD1	(p,p)	0.93	42.16	0.8818	1.071	1.270	1.11	0.69	7.073	1.11	0.69
	(n ,n)	0.58	24.09	0.8992	1.020	1.90	1.11	0.69	3.420	1.11	0.69
	(p,n)	0.73	1.300	0.3351	1.968	1.120	1.11	0.69	0.00	0.00	0.00

Table 10. The best-fit parameters of the folded real potential in addition to Woods-Saxon imaginary potentials to (p,n) data of ^{208}Pb at 35 MeV within different models

Model	Channel	N_R	V MeV	r fm	a fm	W_v MeV	R_v fm	a_v fm	W_s MeV	R_s Fm	a_s fm
OM	(p,p)	-	41.50	1.079	0.848	5.274	1.23	0.69	5.302	1.25	0.69
	(n ,n)	-	9.50	1.080	0.852	5.670	1.24	0.69	6.909	1.25	0.69
	(p,n)	-	1.552	1.076	0.854	2.474	1.04	0.57	0.00	0.00	0.00
DI	(p,p)	0.61	40.50	1.0896	0.8382	5.074	1.25	0.69	5.302	1.25	0.69
	(n ,n)	0.16	8.500	1.0902	0.8320	5.570	1.25	0.69	6.909	1.25	0.69
	(p,n)	0.75	1.352	1.0864	0.8644	2.574	1.01	0.55	0.00	0.00	0.00
DD1	(p,p)	0.55	38.50	1.0896	0.8398	3.074	1.75	0.89	5.302	1.25	0.69
	(n ,n)	0.25	14.50	1.0904	0.8333	3.570	1.55	0.89	6.909	1.25	0.69
	(p,n)	0.85	1.600	1.0864	0.8683	3.974	1.00	0.58	0.00	0.00	0.00
DD3	(p,p)	2.11	37.65	1.0887	0.8468	3.374	1.35	0.89	8.302	1.25	0.69
	(n ,n)	2.44	12.53	1.0936	0.7985	3.800	1.35	0.89	6.909	1.25	0.69
	(p,n)	0.13	0.250	1.0864	0. 867	3.074	1.01	0.55	0.00	0.00	0.00

Table 11. The best-fit parameters of the folded real potential in addition to Woods-Saxon imaginary potentials to (p,n) data of ^{208}Pb at 45 MeV within different models

Model	Channel	N_R	V MeV	r fm	a fm	W_v MeV	R_v fm	a_v fm	W_s MeV	R_s Fm	a_s fm
OM	(p,p)	-	68.60	1.058	0.870	5.59	1.05	0.89	7.38	1.25	0.69
	(n ,n)	-	66.50	1.048	0.862	5.68	1.05	0.89	5.99	1.25	0.69
	(p,n)	-	2.35	1.053	0.858	2.29	1.19	0.79	0.00	0.00	0.00
DI	(p,p)	1.07	68.10	1.0881	0.8506	5.591	1.05	0.89	7.38	1.25	0.69
	(n ,n)	1.29	67.50	1.0889	0.8429	5.680	1.05	0.89	5.99	1.25	0.69
	(p,n)	1.53	2.55	1.0832	0.8881	2.291	1.20	0.79	0.00	0.00	0.00
DD1	(p,p)	1.07	70.61	1.0881	0.8523	5.791	1.01	0.85	7.38	1.25	0.69
	(n ,n)	1.15	65.03	1.0891	0.8455	5.980	1.01	0.85	6.03	1.25	0.69
	(p,n)	0.83	2.723	1.0833	0.8902	2.191	1.20	0.85	0.00	0.00	0.00
DD2	(p,p)	0.85	79.61	1.0882	0.852	3.791	1.20	0.65	7.388	1.25	0.69
	(n ,n)	0.45	36.03	1.0891	0.8458	0.980	1.20	0.65	6.030	1.25	0.69
	(p,n)	0.33	1.523	1.0833	0.890	0.911	1.31	0.75	0.00	0.00	0.00

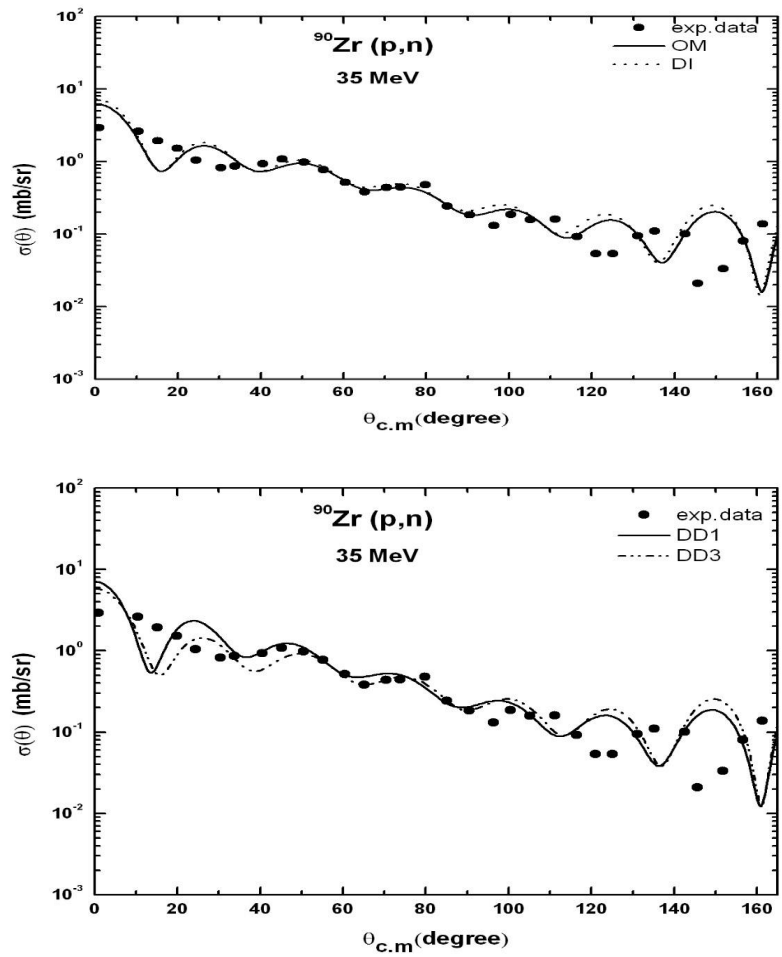

Fig. 2. Quasi-elastic scattering for ^{90}Zr (p,n) at 35 MeV.
The data are taken from Ref. [10]

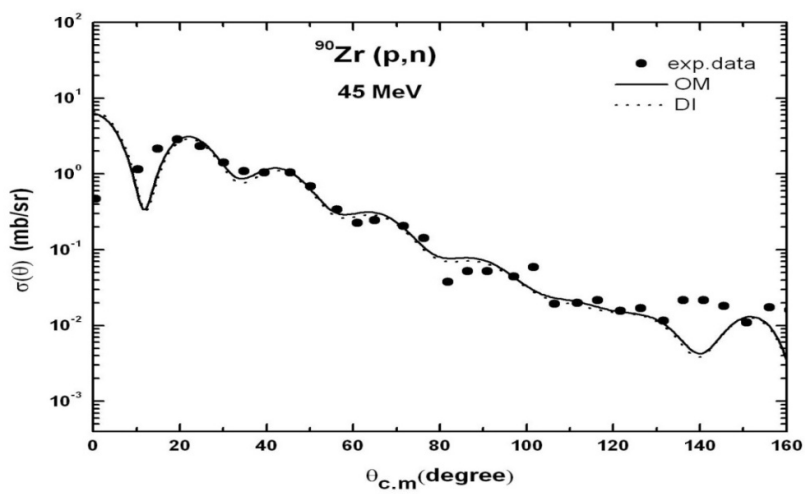

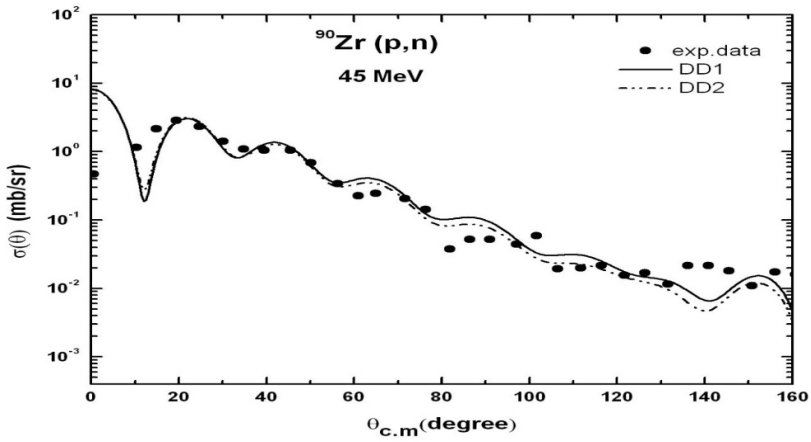

Fig. 3. Quasi-elastic scattering for ^{90}Zr (p,n) at 45 MeV
The data are taken from Ref. [10]

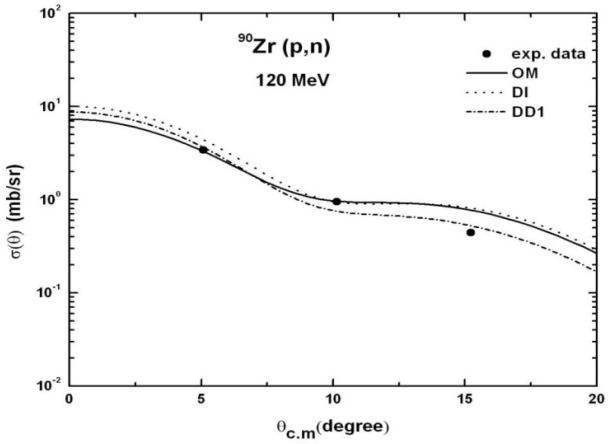

Fig. 4. Quasi-elastic scattering for ^{90}Zr (p,n) at 120 MeV
The data are taken from Ref. [11]

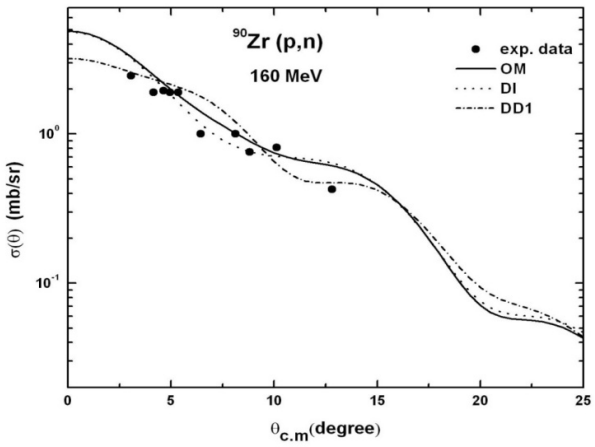

Fig. 5. Quasi-elastic scattering for ^{90}Zr (p,n) at 160 MeV
The data are taken from Ref. [12]

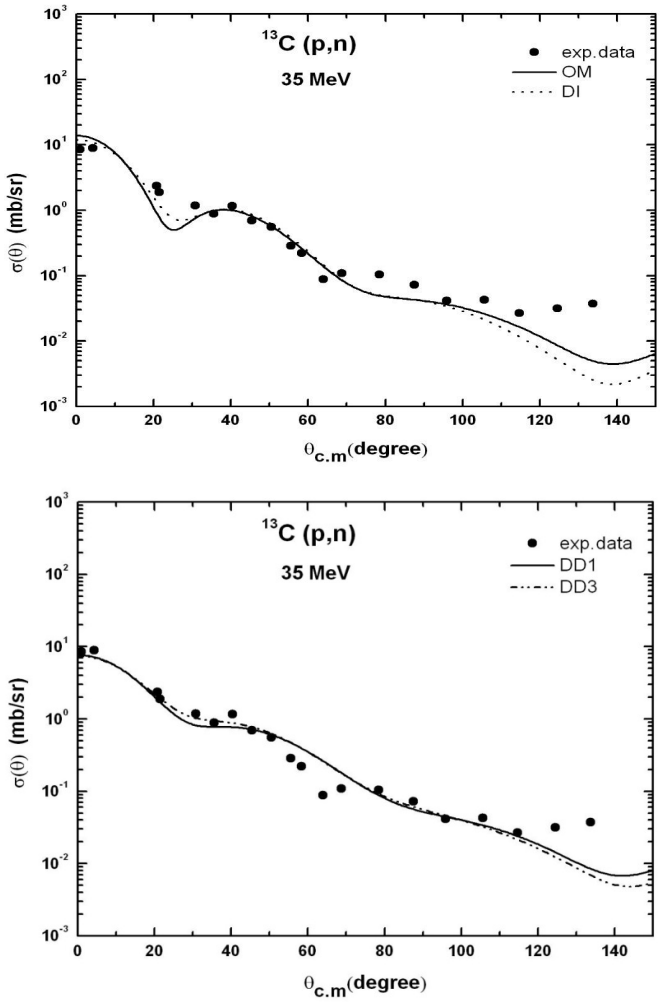

Fig. 6. Quasi-elastic scattering for ^{13}C(p,n) at 35 MeV
The data are taken from Ref. [13,14]

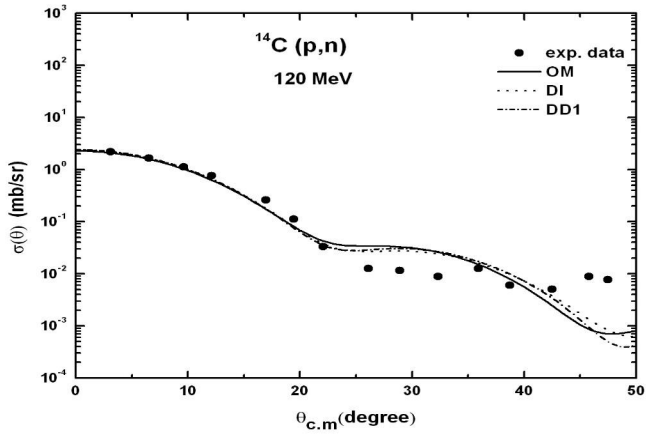

Fig. 7. Quasi-elastic scattering for ^{14}C(p,n) at 120 MeV
The data are taken from Ref. [15]

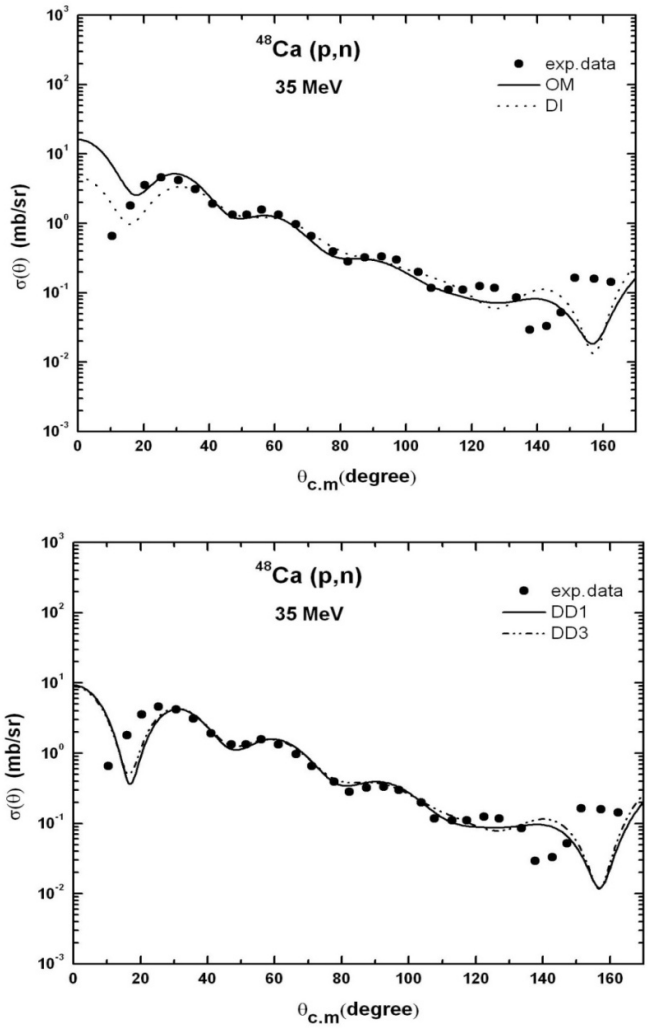

Fig. 8. Quasi-elastic scattering for ^{48}Ca (p,n) at 35 MeV.
The data are taken from Ref. [10]

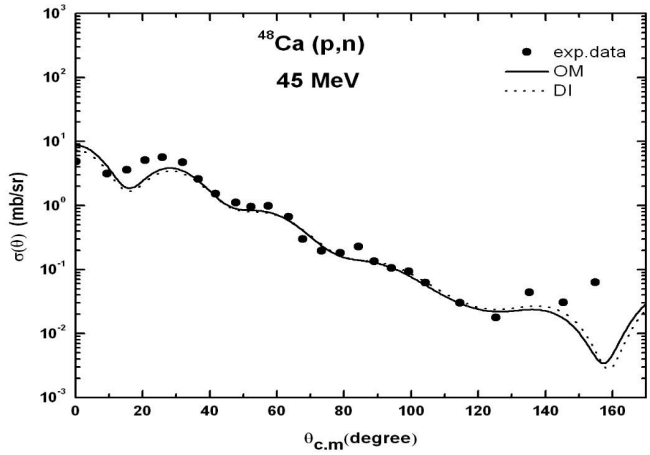

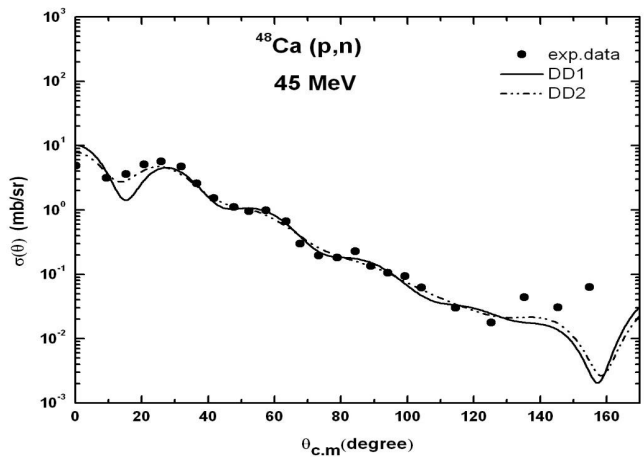

Fig. 9. Quasi-elastic scattering for ^{48}Ca (p,n) at 45 MeV
The data are taken from Ref. [10]

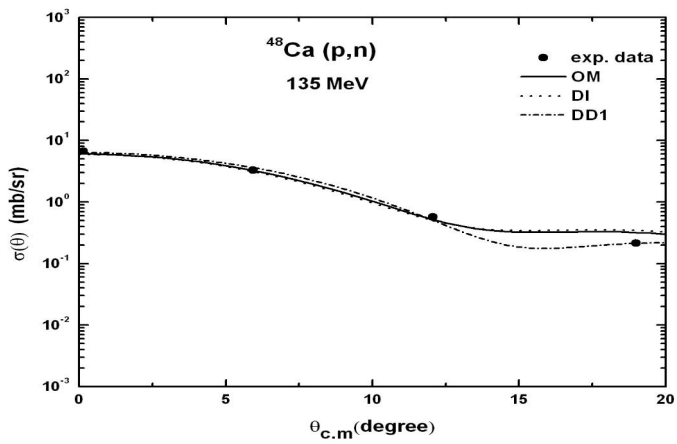

Fig. 10. Quasi-elastic scattering for ^{48}Ca (p,n) at 135 MeV.
The data are taken from Ref. [16]

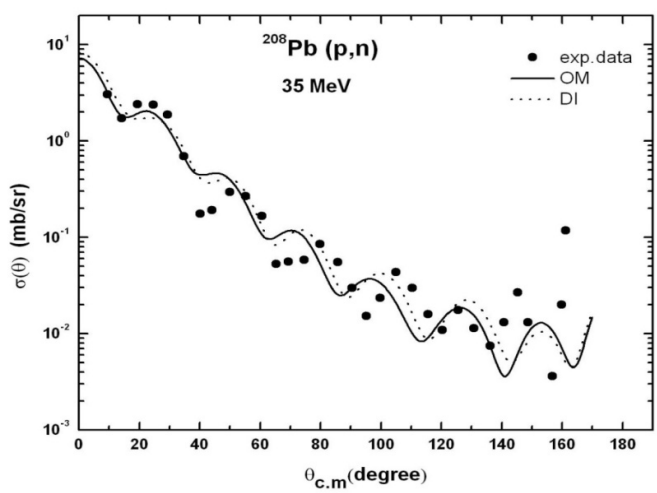

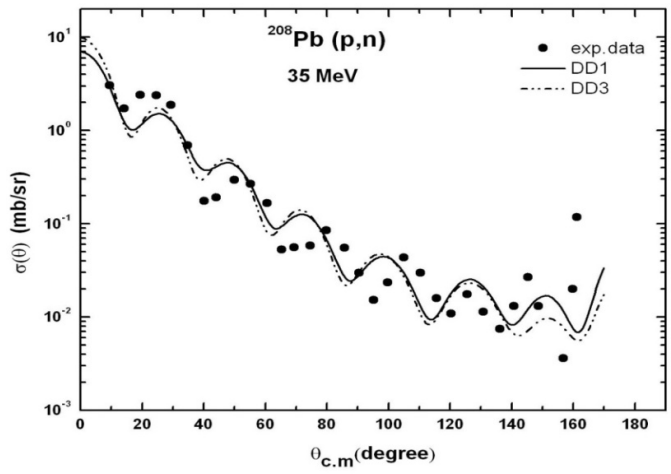

Fig. 11. Quasi-elastic scattering for ^{208}Pb (p,n) at 35 MeV
The data are taken from Ref. [10]

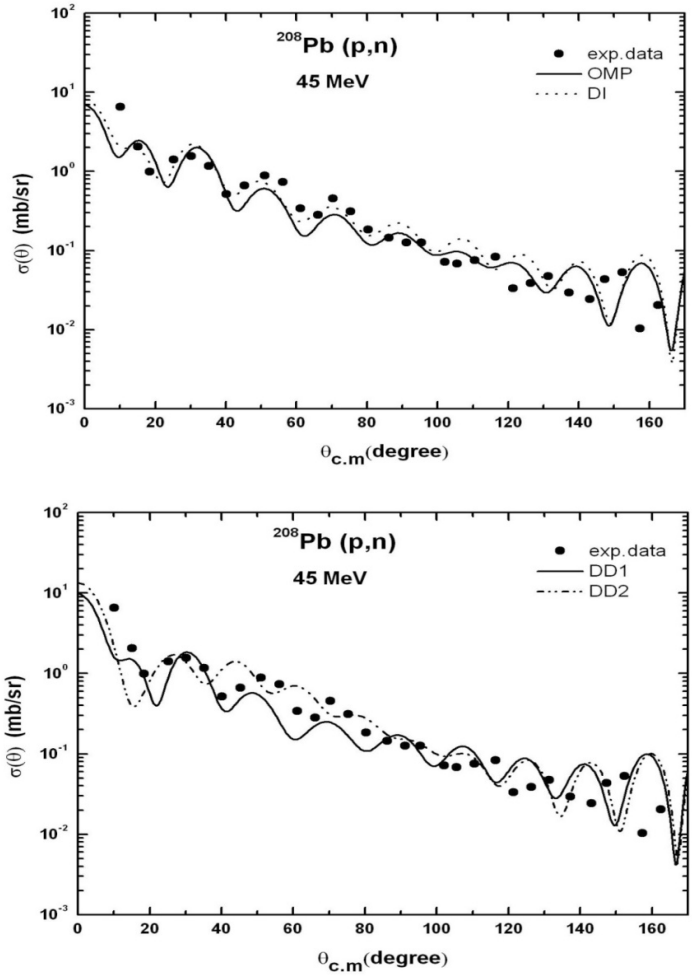

Fig. 12. Quasi-elastic scattering for ^{208}Pb (p,n) at 45 MeV
The data are taken from Ref. [10]

The Figs. 2-12 show the cross section data for the quasi elastic scattering using different potentials for the investigated nuclei at low and high energies. It is easy to notice from these figures that, all the used potentials give a good results in a comparison with others work as in ref. [15,36,37] for the scattering cross sections of each of the reactions (p,n), although these potentials have different characteristic values. This is due to the fact that the calculations of the interaction cross sections depend also up on the imaginary potential.

In harmony with the success of density and energy dependent in the analysis of quasi-elastic scattering (p,n) reaction, it is interested to study how far the calculated Unn and Upp are consistent with Upn in equation (5). So, the calculations were done to get Unn and Upp by changing the potential according to equations (3) and (4). The Unn, Upp and Upn characteristics of the investigated nuclei for the used potentials are presented in Tables 1-11.

5. CONCLUSION

We concluded that using the modified density dependent single folding model successfully describes the quasi-elastic scattering experimental data at different energy ranges and gives a good agreement of the calculated values of Unn and Upp with equation (5).

COMPETING INTERESTS

Authors have declared that no competing interests exist.

REFERENCES

1. Lane AM. Isobaric spin dependence of the optical potential and quasi-elastic (p, n) reactions. Nucl. Phys. 1962;35:676.
2. Carlson JD, Zafiratos CD. Optical model analysis of quasielastic (p, n) reactions at 22.8 MeV. Nucl. Phys. A. 1975;249:29.
3. Satchler GR, Mcvoy KW. Exploratory studies of the elastic scattering of ^{11}Li + ^{12}C. Nucl. Phys. A. 1991;522:621.
4. Arellano HF, von Geramb HV. Extension of the full-folding optical model for nucleon-nucleus scattering with applications up to 1.5 GeV. Phys. Rev. C. 2002;66:24602.
5. Ogloblin AA, Aglukhov Yu. New measurement of the refractive, elastic ^{16}O + ^{12}C scattering at 132, 170, 200, 230 and 260 MeV incident energies. Phys. Rev. C. 2000;62:44601.
6. Dao T. Khoa, Satchler GR. Generalized folding model for elastic and inelastic nucleus–nucleus scattering using realistic density dependent nucleon–nucleon interaction. Nucl. Phys. A. 2000;668:3.
7. El-Nohy NA, Motaweh HA, Attia A, El-Hammamy MN. The relation between the isoscalar and isovector interaction potentials. 20th International Seminar on Interaction of Neutrons with Nuclei: Alushta, Ukraine, 21–26 May; 2012.
8. Kunz PD. Instructions for the use of DWUCK4: A distorted wave born approximation program, COO-535-606, Abstract number NESC9872, 36; 1987.
9. Cook J. DFPOT - a program for the calculation of double folded potentials. Comput. Phys. Comm. 1982;25:125.
10. Doering RR, Patterson DM, Galonsky A. Microscopic description of isobaric-analog-state transitions induced by 25-, 35-, and 45-MeV protons. Phys. Rev. C. 1975;12: 378.
11. Bainum DE, Rapaport J, Goodman CD, et al. Observation of giant particle-hole resonances in ^{90}Zr(p, n)^{90}Nb. Phys. Rev. Lett. 1980;44:1751.
12. Sugarbaker E, et al. Proceedings of the International Conference on Nuclear Structure, Amsterdam, edited by A. Van Der Wonde and B. J. Verhaar. 1982;77. Jacob Rapaport (Private Communication).
13. Orihara H, Murakami T. The neutron time-of-flight facility at Tohoku University cyclotron. Nucl. Instrum. Methods. 1981;181:15.
14. Orihara H, et al. Status of the cyric neutron TOF facilities upgrade. Nucl. Instrum. Methods Phys. Res. 1987;A257:189.
15. Jacob Rapaport, Unpublished (Private Communication); H. F. Arellano, W. G. Love. An in-medium full-folding model approach to quasi-elastic (p,n) charge–exchange reactions. arXiv: 0706.2523 v1 [nucl-th]; 2007.
16. Anderson BD, Mostajabodda'vati M, Lebo C, et al. Isobaric-analog-state transitions in the (p,n) reaction at 135 MeV and density-dependent impulse-approximation calculations. Phys. Rev. C. 1991;43:1630.
17. Becheetti FD, Greenlees GW. Nucleon-nucleus optical-model parameters, A>40, E<50 MeV. Phys. Rev. 1969;182:1190.
18. Varner RL, Thompson WJ, McAbee TL, Ludwig EJ, Clegg TB. A global nucleon

optical model potential. Phys. Rep. 1991;201:57.
19. Koning AJ, Delaroche JP. Local and global nucleon optical models from 1 keV to 200 MeV. Nucl. Phys. A. 2003;713:231.
20. Satchler GR, Love WG. Folding model potentials from realistic interactions for heavy-ion scattering. Phys. Rep. 1979;55: 183.
21. Bohlen HG, Clover MR, Ingold G, et al. Observation of the nuclear rainbow scattering for $^{12}C+^{12}C$ at E_{Lab} =300 MeV. Z. Phys. A. 1982;308:121.
22. Bohlen HG, Chen XS, Cramer JG, et al. Refractive scattering and the nuclear rainbow in the interaction of $^{12, 13}C$ with ^{12}C at 20 MeV/N. Z. Phys. A. 1985;322:241.
23. Stiliaris E, Bohlen HG, Frobrich P, et al. Nuclear rainbow structures in the elastic scattering of ^{16}O on ^{16}O at E_L =350 MeV. Phys. Lett. B. 1989;223:291.
24. Basu DN, Roy Chowdhury P, Samanta C. Equation of state for isospin asymmetric nuclear matter using lane potential. Acta Phys. Pol. B. 2006;37(10):2869.
25. Myers WD. Geometric properties of leptodermous distributions with applications to nuclei. Nucl. Phys. A. 1973;204:465.
26. Bandyopadhyay D, Samanta C, Samaddar SK, De JN. Thermostatic properties of finite and infinite nuclear systems. Nucl. Phys. A. 1990;511:1.
27. Roy Chowdhury P, Samanta C, Basu DN. Modified Bethe-Weizsacker mass formula with isotonic shift and new drip lines. Mod. Phys. Letts. A. 2005;21:1605.
28. Audi G, Wapstra AH, Thibault C. The AME2003 atomic mass evaluation: (II). Tables, graphs and references. Nucl. Phys. A. 2003;729:337.
29. Satpathy L, Uma Maheswari VS, Nayak RC. Finite nuclei to nuclear matter: A leptodermous approach. Phys. Rep. 1999;319:85.
30. Schutz Y, et al. The role of nuclear incompressibility in the production of hard photons in heavy-ion collisions. Nucl. Phys. A. 1996;599:97c.
31. Friedman B, Pandharipande VR. Hot and cold, nuclear and neutron matter. Nucl. Phys. A. 1981;361:502.
32. Ozawa A, et al. Nuclear size and related topics. Nucl. Phys. A. 2001;691: 599.
33. De Veries H, De Jager CW. Nuclear charge and magnetization density distribution parameters from elastic electron scattering. Nucl. Data Tables. 1987;36:495.
34. El-Azab Farid M, Hassanain MA. Density - independent folding analysis of the Li-6, Li-7 elastic scattering at intermediate energies. Nucl. Phys. A. 2000;678:39.
35. Umemoto Y, Hirenzaki S, Kume K, Toki H. Isotope dependence of deeply bound pionic states in Sn and Pb. Phys. Rev. C. 2000;62:024606.
36. Osman A. Density dependent nucleon-nucleus optical potential in the (p,n) reactions. Acta Phys. Pol. B. 2009;40: 2345.
37. Khoa DT, Than HS, Cuong DC. Folding model study of the isobaric analog excitation: Isovector density dependence, Lane potential, and nuclear symmetry energy. arXiv: 0706.1282 v1 [nucl-th]; 2007.

Peer-review history:
The peer review history for this paper can be accessed here:
https://sdiarticle4.com/review-history/52078